© 2020. Published by The Company of Biologists Ltd | Development (2020) 147, dev192070. doi:10.1242/dev.192070

RESEARCH ARTICLE

Retinoic acid synthesis and autoregulation mediate zonal patterning of vestibular organs and inner ear morphogenesis

Kazuya Ono[1], Lisa L. Sandell[2], Paul A. Trainor[3,4] and Doris K. Wu[1,*]

ABSTRACT

Retinoic acid (RA), a vitamin A (retinol) derivative, has pleiotropic functions during embryonic development. The synthesis of RA requires two enzymatic reactions: oxidation of retinol into retinaldehyde by alcohol dehydrogenases (ADHs) or retinol dehydrogenases (RDHs); and oxidation of retinaldehyde into RA by aldehyde dehydrogenases family 1, subfamily A (ALDH1as), such as ALDH1a1, ALDH1a2 and ALDH1a3. Levels of RA in tissues are regulated by spatiotemporal expression patterns of genes encoding RA-synthesizing and -degrading enzymes, such as cytochrome P450 26 (Cyp26 genes). Here, we show that RDH10 is important for both sensory and non-sensory formation of the vestibule of the inner ear. Mice deficient in *Rdh10* exhibit failure of utricle-saccule separation, otoconial formation and zonal patterning of vestibular sensory organs. These phenotypes are similar to those of *Aldh1a3* knockouts, and the sensory phenotype is complementary to that of *Cyp26b1* knockouts. Together, these results demonstrate that RDH10 and ALDH1a3 are the key RA-synthesis enzymes involved in vestibular development. Furthermore, we discovered that RA induces *Cyp26b1* expression in the developing vestibular sensory organs, which generates the differential RA signaling required for zonal patterning.

KEY WORDS: RDH10, CYP26b1, ALDH1a3, Retinoic acid, Striola, Patterning

INTRODUCTION

Retinoic acid (RA) is a derivative of the fat-soluble vitamin A (retinol), which has pleiotropic functions during embryogenesis (Ross et al., 2000) and into adulthood (Anderson et al., 2008; Jacobs et al., 2006). RA controls gene expression at the transcriptional level through interaction with heterodimers of nuclear RA receptors (RARs) and retinoid X receptors (RXRs) that bind to the RA response elements (RAREs) in target genes. RA is synthesized *de novo* from retinol via two enzymatic reactions, one of which is mediated by alcohol dehydrogenases or retinol dehydrogenases (ADHs/RDHs), whereas the other is mediated by aldehyde dehydrogenases (ALDHs). Gradients of RA are established and mediated by diffusion of RA combined with the action of RA-degrading enzymes, encoded by cytochrome P450 26 (*Cyp26a1*), *Cyp26b1* and *Cyp26c1*. The spatial and temporal regulation of *Aldh1a* and *Cyp26b1* gene expression are known to be important for tissue organogenesis, such as the hindbrain (Hernandez et al., 2007), limb (Sakai et al., 2001; Yashiro et al., 2004), eye (da Silva and Cepko, 2017; Molotkov et al., 2006) and inner ear (Bok et al., 2011). Notably, RA synthesis mediated by ALDH1a3 is required for inner ear morphogenesis and formation of otoconia, which are accessory structures of the vestibular otolithic organs that optimize the detection of sensory inputs (Romand et al., 2013). However, the enzyme (or enzymes) that generates the retinaldehyde substrate for ALDH1a3 during RA synthesis has not been defined. There are at least five ADH/RDH enzymes (ADH1, ADH3, ADH4, RDH1 and RDH10) that could play a role in the generation of retinaldehyde, the substrate for ALDH1a proteins (Duester, 2008; Kumar et al., 2012). Evidence suggests that RA signaling is regulated at the level of retinol oxidation, which is primarily mediated by RDH10 during embryogenesis (Farjo et al., 2011; Metzler and Sandell, 2016; Sandell et al., 2012). Mouse mutants that lack *Rdh10* or harbor a hypomorphic form of *Rdh10*, $Rdh10^{trex}$, show defects in the formation of multiple organs, including abnormal patterning of the hindbrain and a smaller or duplicated inner ear primordium (Rhinn et al., 2011; Sandell et al., 2012, 2007). The potential roles of RDH10 in later stages of inner ear development, however, have not been explored.

The vestibular system of the inner ear comprises five sensory organs: two otolithic organs, the utricle and the saccule, each of which contains a sensory tissue macula that detects linear acceleration, and three ampullae, which house the cristae that detect angular velocity (Fig. 1A). The sensory epithelium within each vestibular organ consists of type I and type II hair cells (HCs) that are surrounded by supporting cells and innervated by afferent nerve endings. Each vestibular sensory epithelium contains a specialized and conserved region known as the striola in the maculae of the utricle and saccule, and the central zone in semicircular canal cristae (Fig. 1A). Striolar/central zones have distinct anatomical and functional features, such as the presence of larger type I HC somata innervated by pure/complex calyceal nerve endings, each of which can encase two or three HC bodies. These neurons are characterized by an irregular firing pattern (Eatock and Songer, 2011). Such specialized central regions are important for evoking short-latency compound action potentials, known as vestibular evoked potentials, in response to transient linear acceleration (Jones et al., 2015; Ono et al., 2020).

Recently, we showed that differential levels of RA are required for patterning of the striolar/central versus extrastriolar/peripheral zone (Ono et al., 2020). *Cyp26b1* is expressed in the presumptive striolar/central zone, and mice deficient in *Cyp26b1* lack many features of these specialized regions and exhibit a severe reduction in striolar type I HCs and complex calyces (Fig. 1B). The RA required for patterning of the vestibular organs is largely supplied by the activity of the enzyme ALDH1a3, which is predominantly expressed in the extrastriolar/peripheral zone. In contrast to the *Cyp26b1* mutants, $Aldh1a3^{-/-}$ embryos show an expanded striola at the expense of the

[1]National Institute on Deafness and Other Communication Disorders, National Institutes of Health, Bethesda, MD 20892, USA. [2]Department of Oral Immunology and Infectious Diseases, School of Dentistry, University of Louisville, Louisville, KY 40201, USA. [3]Stowers Institute for Medical Research, Kansas City, MO 64110, USA. [4]Department of Anatomy and Cell Biology, University of Kansas Medical Center, Kansas City, KS 66160, USA.

*Author for correspondence (wud@nidcd.nih.gov)

K.O., 0000-0002-3857-0055; L.L.S., 0000-0002-1735-8223; P.A.T., 0000-0003-2774-3624; D.K.W., 0000-0002-1400-3558

Handling Editor: Patrick Tam
Received 27 April 2020; Accepted 1 July 2020

Development (2020) 147, dev192070. doi:10.1242/dev.192070

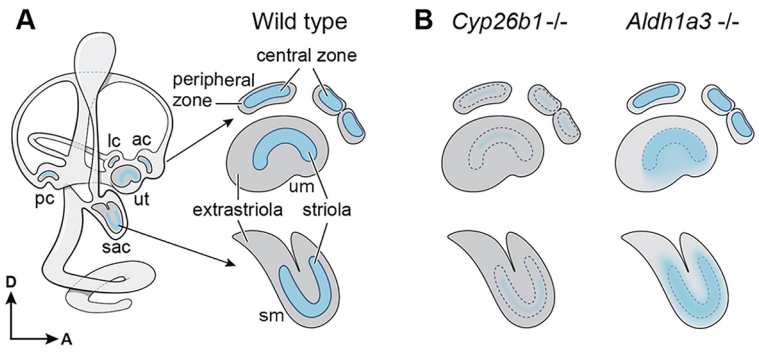

Fig. 1. Schematic diagram of the inner ear and its vestibular organs in wild type and mutants. (A) Each vestibular sensory epithelium of the inner ear consists of a specialized region (blue shading) known as the striola in the maculae of the utricle and saccule and the central zone in the cristae. The striola and central zone express *Cyp26b1*, a gene encoding an RA-degrading enzyme, whereas the extrastriola and peripheral zone (gray shading) express *Aldh1a3*, a gene encoding an RA-synthesizing enzyme. (B) In *Cyp26b1* knockouts, the striolar/central zone is severely reduced. By contrast, in *Aldh1a3* knockouts, the striola is expanded but the central zone remains normal. ac, anterior crista; lc, lateral crista; pc, posterior crista; sac, saccule; sm, saccular macula; um, utricular macula; ut, utricle. Orientations: A, anterior; D, dorsal.

extrastriola in the maculae of the utricle and saccule; however, the central zones in cristae appear normal (Fig. 1B; Ono et al., 2020). Additionally, these mutants exhibit various morphogenetic defects, such as a severe reduction in otoconia and a failure to separate the utricle and saccule (Romand et al., 2013). Despite these established roles of the enzyme ALDH1a3 in vestibular formation, the ADH/RDH enzyme (or enzymes) that provides the substrate for ALDH1a3 during inner ear development remains unknown.

In the present study, we show that *Rdh10* is expressed in the embryonic vestibular organs. Inner ear-specific deletion of *Rdh10* largely phenocopies the defects reported in *Aldh1a3* knockouts, including fusion of the utricle and saccule, absence of the otoconia and expansion of striolar/central zone-specific genes. These results indicate that retinaldehyde, the substrate for ALDH1a3, is primarily generated by the enzymatic function of RDH10 during vestibular development. Additionally, we show that RA in the developing vestibular organs upregulates its own degrading enzyme, *Cyp26b1*, indicating that the level of RA is autoregulated.

RESULTS

Rdh10 expression during inner ear development

RA produced by the catalytic activity of ALDH1a3 is important for vestibular development (Ono et al., 2020; Romand et al., 2013); however, the enzyme (or enzymes) required for production of retinaldehyde, the ALDH1a3 substrate, remain unknown. We investigated the inner ear expression pattern of *Rdh10*, which is one of the enzymes that catalyzes the production of the retinaldehyde, the substrate required by ALDH1a3. At embryonic day (E) 15.5, *Rdh10* is strongly expressed in the endolymphatic sac (Fig. 2A) and duct (Fig. 2C). This expression extends beyond the separation between the utricle and saccule (Fig. 2C, asterisk) to where the endolymphatic duct enters the saccule (Fig. 2E, asterisk) (Romand et al., 2008). A similar pattern of *Rdh10* expression has been reported in the inner ear at E12.5 (Romand et al., 2008), and notably, *Rdh10* expression in the endolymphatic duct and sac colocalize with *Aldh1a3* (Fig. 2B,D,F). In the sensory tissues, *Aldh1a3* expression is weak in the striola (Fig. 2D,F, bracket), but its expression in the extrastriolar region of utricular and saccular maculae and in the peripheral zone of the semicircular canal cristae is robust (Fig. 2D,F; Ono et al., 2020). By contrast, *Rdh10* expression is weakly detected in the extrastriolar sensory region (Fig. 2C, arrows). Overall, the similarity of expression patterns between *Rdh10* and *Aldh1a3* in the developing vestibular system suggests that RDH10 could be involved in the generation of RA for vestibular formation.

Utricle and saccule fail to separate in *Rdh10* conditional knockouts

In *Aldh1a3*$^{-/-}$ embryos, the utricle and saccule are fused, and the otoconia are either misshapen or missing (Romand et al., 2013). We asked whether RDH10 is required for generation of the ALDH1a3 substrate retinaldehyde during vestibular development. *Rdh10*$^{-/-}$ mutants die at mid-gestation (Rhinn et al., 2011; Sandell et al., 2012, 2007). To circumvent early embryonic lethality of *Rdh10*$^{-/-}$, conditional knockouts of *Rdh10* (*Rdh10* cKO) were generated using *Foxg1*^{Cre} (Hébert and McConnell, 2000), in which Cre recombinase is activated in the otocyst.

In wild-type inner ears, the membranous labyrinth is partitioned into two chambers by E16.5, separated at the utricle and saccule (Cantos et al., 2000). This separation of the labyrinth into two compartments is evidenced by the fact that a single injection of paint solution into the cochlear duct fills only the cochlear duct,

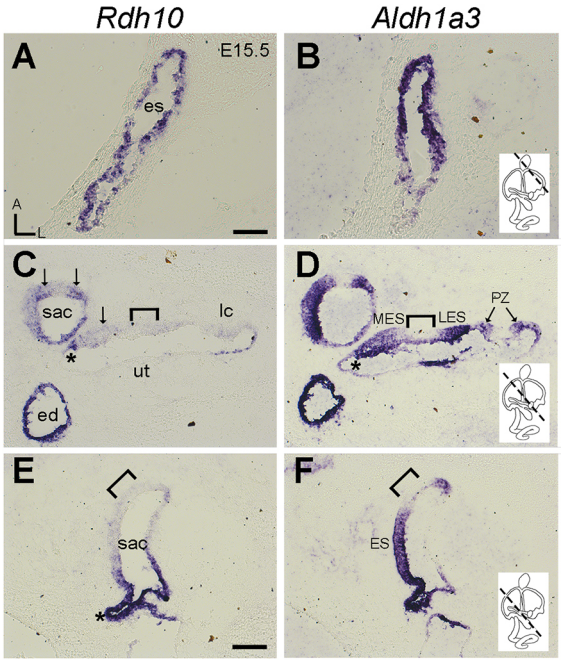

Fig. 2. Expression of *Rdh10* in the developing inner ear. (A-F) Adjacent sections of E15.5 vestibule showing the expression pattern of *Rdh10* and *Aldh1a3*. (A,B) Both *Rdh10* (A) and *Aldh1a3* (B) are expressed in the endolymphatic sac (es). (C,D) Colocalization of *Rdh10* (C) and *Aldh1a3* (D) hybridization signals in the endolymphatic duct (ed), medial non-sensory region of the utricle (*) and part of the maculae of the utricle and saccule (arrows). (E,F) Colocalization of *Rdh10* (E) and *Aldh1a3* (F) hybridization signals where the endolymphatic duct meets the saccule (*). Dashed lines in schematic diagrams of the inner ear (B,D,F) indicate approximate levels of sections. Bracket represents part of the striola in the maculae of the utricle and saccule, which is devoid of *Aldh1a3* expression, but its expression in the extrastriolar regions (MES, LES and ES) and peripheral zone (PZ) is robust. ES, extrastriola; lc, lateral crista; LES, lateral extrastriola; MES, medial extrastriola; PZ, peripheral zone; sac, saccule; ut, utricle. Orientations: A, anterior; L, lateral. Scale bars: 200 µm in A, which applies to A-D; 100 µm in E.

Development (2020) 147, dev192070. doi:10.1242/dev.192070

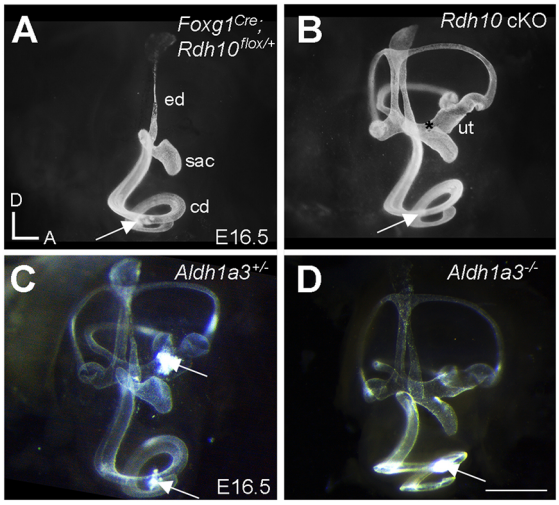

Fig. 3. Failure of the utricle and saccule to separate in *Rdh10* cKO and *Aldh1a3*$^{-/-}$ mutant ears. (A-D) Lateral views of the paint-filled, right inner ears at E16.5. (A) A single injection of paint solution into the cochlea (arrow) filled only the cochlear duct (cd), saccule (sac) and endolymphatic duct (ed) and endolymphatic sac in *Foxg1*^{Cre}; *Rdh10*$^{flox/+}$ controls. (B) A single injection of paint solution into a similar location in *Rdh10* cKO (arrow) filled the entire membranous labyrinth owing to failure of the utricle (ut) and saccule to separate (*). (C,D) Compared with the *Aldh1a3*$^{+/-}$ control (C), which requires two injections (arrows) to fill the membranous labyrinth, a single injection into the cochlear duct (arrow) fills the entire labyrinth in *Aldh1a3*$^{-/-}$ inner ear (D). A and B are siblings from the same litter and likewise for C and D. Orientations: A, anterior; D, dorsal. Scale bar: 1 mm.

saccule, endolymphatic sac and duct (Fig. 3A), whereas filling of the remaining utricle, semicircular canals and cristae requires a separate injection into the utricle (Cantos et al., 2000). Failure of this utricle-saccule separation occurs in *Aldh1a3*$^{-/-}$ mutants (Romand et al., 2013). Our paint filling results confirmed the utricle-saccule fusion phenotype in the *Aldh1a3*$^{-/-}$ inner ear; the entire labyrinth of *Aldh1a3*$^{-/-}$ mutants was filled by a single injection into the cochlear duct (Fig. 3D, arrow), whereas control littermates required two injections (Fig. 3C, arrows). Similar to *Aldh1a3*$^{-/-}$ ears, a single injection of paint solution into the cochlear duct of *Rdh10* cKO mutants filled the entire labyrinth (Fig. 3B), which is indicative of failure of separation between the utricle and saccule. Together, these results suggest that RDH10 and ALDH1a3, which are involved in the synthesis of RA, are each required for proper separation of the utricle and saccule during vestibular development.

Absence of otoconia in *Rdh10* conditional knockouts

Otoconia are composed of calcium carbonate crystals that overlie HCs in the maculae of the utricle and saccule. Mutant mice that lack otoconia fail to swim (Paffenholz et al., 2004), and a prominent phenotype of *Aldh1a3*$^{-/-}$ mutants is a significant loss of otoconia and swimming ability (Romand et al., 2013). In dissected utricles, otoconia are clearly evident on visual inspection; they appear as a whitish layer on top of the sensory epithelium (Fig. 4A). The central region, corresponding to the location of the striola, appears clear (Fig. 4A, arrow), owing to the smaller number and size of the otoconia in this region. The whitish opaque otoconial layer was absent (Fig. 4B, n=12/13) or reduced in number (n=1/13) in utricular maculae of *Aldh1a3*$^{-/-}$ mutants. The otoconia were also absent in *Rdh10* cKO embryos (Fig. 4C, n=9/9). Together, these results indicate that RDH10 and ALDH1a3 are each required for otoconial formation.

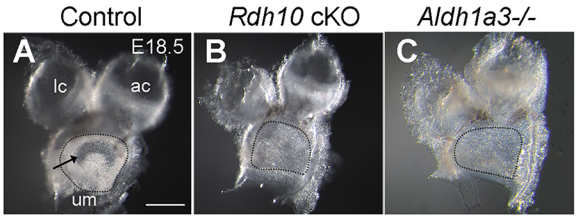

Fig. 4. Absence of otoconia in the utricular macula of *Rdh10* cKO and *Aldh1a3*$^{-/-}$ mutants. (A-C) Dissected utricular macula (um), anterior crista (ac) and lateral crista (lc) from a control (A), *Aldh1a3*$^{-/-}$ (B) and *Rdh10* cKO (C) ear at E18.5. Dotted lines outline the surface of the um that is not obscured by the remaining tissues from the roof of the utricle. (A) In the control, the whitish and opaque otoconia on the surface of the um are apparent, with a central clear area corresponding to the position of the striola (arrow). In comparison to the control (A), these whitish otoconia are missing in maculae of both *Rdh10* cKO (B) and *Aldh1a3*$^{-/-}$ (C) utricles (compare among regions within the dotted lines). Scale bar: 200 µm.

Increased striolar/central zone in *Rdh10* conditional knockouts

In addition to the functions of ALDH1a3 in morphogenesis of the vestibular system and formation of the otoconia, it is also required for zonal patterning of the vestibular organs (Ono et al., 2020). Lack of *Aldh1a3* causes an expanded striola-like region in the maculae of the utricle and saccule, but the central zones of the cristae are not affected (Fig. 1; Ono et al., 2020). To determine whether RDH10 has a similar role in patterning the vestibular organs, we examined the Ca^{2+}-binding protein oncomodulin (Ocm) in the vestibular organs of *Rdh10* cKO mutant mice, because Ocm is expressed exclusively in type I HCs of the striolar/central zone (Simmons et al., 2010). In contrast to controls (Fig. 5A,A′,C,C′), the number of Ocm^{+} HCs was increased in the maculae of *Rdh10* cKO utricles and saccules (Fig. 5B,B′,D-F). Both maculae contain two distinct regions that are separated by the line of polarity reversal (LPR). Stereociliary bundles atop HCs are arranged in opposite orientations on either side of this LPR. In the utricular macula, the striola defined by Ocm expression is medial to the LPR, which is determined by the position of the kinocilium, indicated by the absence of anti-spectrin antibody staining (Fig. 5H,H′,L). In the utricular macula of *Rdh10* cKO mutants, the domain of Ocm expression was expanded medially but not laterally from the LPR (Fig. 5I,I′,L), whereas in the saccular macula, expanded Ocm expression was evident on both sides of the LPR (Fig. 5J,K,M). The phenotype in *Rdh10* cKO mutants was largely comparable to the phenotype observed in *Aldh1a3*$^{-/-}$ ears (Ono et al., 2020). However, unlike *Aldh1a3*$^{-/-}$ ears, *Rdh10* cKO cristae also showed an increase in Ocm^{+} HCs (Fig. 5B,B′,G). These results indicate that RDH10 is important for the establishment of extrastriolar/peripheral zones of all vestibular organs. Furthermore, the phenotypic similarities between *Aldh1a3*$^{-/-}$ and *Rdh10* cKO mutants indicate that RDH10 and ALDH1a3, which execute the two sequential enzymatic reactions that generate RA, regulate vestibular development.

Regulation of *Cyp26b1* by RA signaling

We previously demonstrated that degradation of RA by *Cyp26b1* is required for the formation of the striolar/central zones of vestibular sensory organs (Ono et al., 2020). A remaining puzzle is the mechanism (or mechanisms) that regulate expression of *Cyp26b1*. Given that RA mediates negative feedback by inducing its own degrading enzymes (Cyp26 genes) in other systems, such as the retina and vasculature system (da Silva and Cepko, 2017; Reijntjes et al., 2005), we asked whether *Cyp26b1* expression is also

Development (2020) 147, dev192070. doi:10.1242/dev.192070

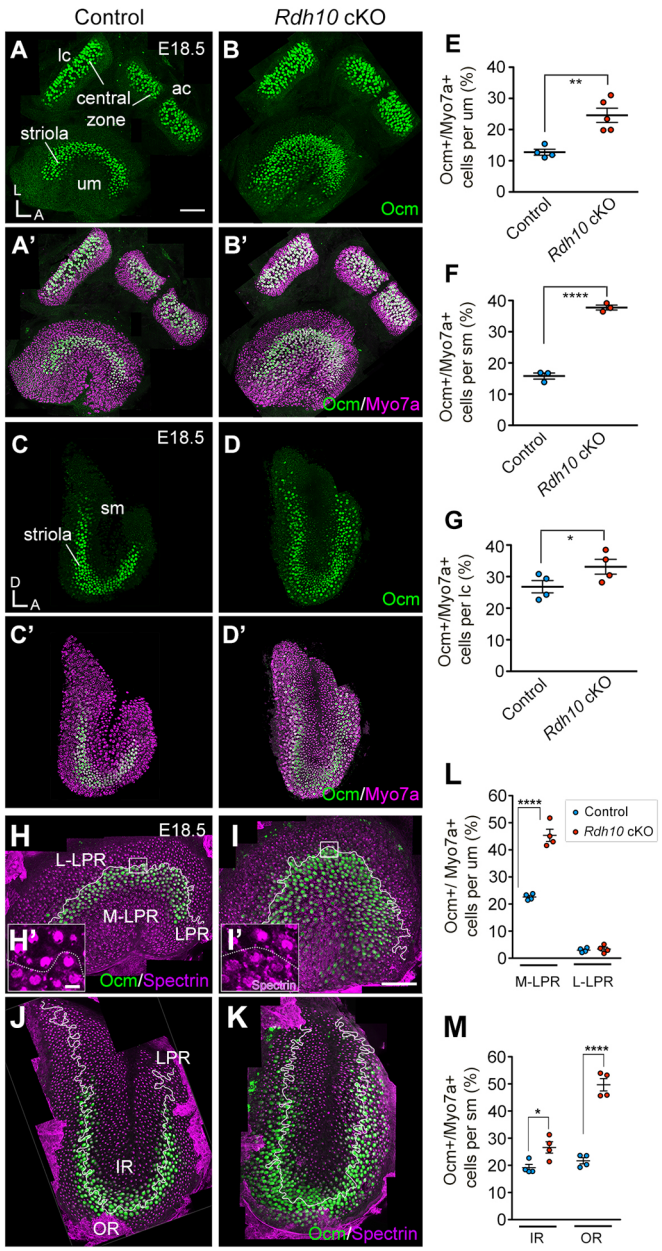

Fig. 5. Increased Ocm expression in *Rdh10* cKO mutants. (A-G) Immunohistochemistry of myosin VIIA (Myo7a; magenta) and oncomodulin (Ocm; green) (A-D′) and quantification of percentages of Ocm$^+$ HCs (E-G) in utricular macula (um), lateral crista (lc) and saccular macula (sm). In *Rdh10* cKO, Ocm$^+$ HCs are increased in the um (24.5±2.5% per um, *n*=5, *P*=0.0034, Student's unpaired *t*-test; B,B′,E), sm (37.7±1.0% per sm, *n*=3, *P*=0.000062; D,D′,F) and lateral crista (34.1±3.2% per lc, *n*=5, *P*=0.0394; B,B′,G) when compared with the control um (12.7±0.9%, *n*=4; A,A′,E), sm (15.8±1.2%, *n*=3; C,C′,F) and lateral crista (26.7±2.7%, *n*=4; A,A′,G), respectively. (H-M) Immunohistochemistry of Ocm (green) and β-spectrin (magenta) (H-K) and quantification of Ocm$^+$ HCs (L,M) in regions of um and sm at E18.5. (H,H′,L) In control utricles, most Ocm$^+$ HCs (green) are located in the region medial (M-LPR, 22.6±0.6% per um, *n*=4) but not lateral (L-LPR, 3.0±0.4%, *n*=4) to the line of polarity reversal (LPR, white lines). Hair bundle orientations are determined by the position of the kinocilium, which is devoid of β-spectrin staining (H′). (I,I′,L) Ocm$^+$ HCs are increased in the medial (45.3±2.2%, *n*=4, *P*=0.000065, Student's unpaired *t*-test) but not lateral region (3.3±0.7%, *n*=4, *P*=0.644) of *Rdh10* cKO um. (J,M) In controls, the LPR (white line) bisects the striola, and Ocm is expressed in the inner (IR, 19.2±1.2% per sm, *n*=4) and outer (OR, 21.7±1.1%, *n*=4) regions of the sm. (K,M) The Ocm$^+$ domain is expanded to both the IR (26.6±2.1%, *n*=4, *P*=0.021) and the OR (49.7±2.3%, *n*=4, *P*=0.000032) of *Rdh10* cKO sm. **P*<0.05, ***P*<0.01, *****P*<0.0001. Error bars: s.e.m. Orientations: A, anterior; D, dorsal; L, lateral. Scale bars: 200 µm in A,I; 20 µm in H′.

regulated by RA in the developing vestibular organs. Towards that end, an *in vitro* explant culture of the utricular macula and two cristae was established (Fig. 6A), and we tested the effects of RA treatments on *Cyp26b1* expression (Ono et al., 2020). We found that *Cyp26b1* was upregulated in E14.5-E15.0 utricular explants 16 h after RA treatment in a dose-dependent manner (Fig. 6B-D). Within an hour of the *in situ* hybridization reaction, *Cyp26b1* expression was already upregulated and expanded towards the periphery in RA-treated samples (Fig. 6C,D), whereas a hybridization signal was not detectable in the control (Fig. 6B) until after 3 h (Fig. 6B′). These results suggest that RA might induce *Cyp26b1* expression in the vestibular organs.

Deletion of *Cyp26b1 in vivo* reduces Ocm expression in the striola and central zone, and this phenotype is likely to be caused by augmented RA signaling (Ono et al., 2020). We therefore examined whether RA inhibits Ocm expression in cultured utricular maculae (Fig. 6A). Ocm expression is evident in the mouse macula at ~E16.0 (McInturff et al., 2018). After culturing E14.5-E15.0 vestibular explants for 3 days in RA-free medium, Ocm$^+$ HCs were present in the presumptive striola of the utricular macula and central zones of the cristae (Fig. 6E). By contrast, Ocm$^+$ HCs were absent in RA-treated utricular maculae and lateral cristae (Fig. 6F-H), suggesting that exogenous RA inhibits Ocm expression. These results are consistent with the reduced Ocm expression in the *Cyp26b1*$^{-/-}$ mutants and support the hypothesis that RA signaling is augmented in these mutants (Ono et al., 2020). Taken together, these results suggest that despite upregulation of *Cyp26b1* expression by RA (Fig. 6B-D), exogenous RA overrides endogenous CYP26b1 activity *in vitro* and causes a RA gain-of-function phenotype.

The above *in vitro* results suggest that homeostatically regulated RA levels, mediated in part by RA-responsive *Cyp26b1* expression, are important for formation of the striola and central zone. We tested this hypothesis further by examining *Cyp26b1* expression in *Aldh1a3*$^{-/-}$ mutants, in which striolar properties of otolith organs are increased and, presumably, RA signaling is severely reduced (Ono et al., 2020). Compared with controls, *Tectb* which labels striolar supporting cells, was increased in the macula of *Aldh1a3*$^{-/-}$ utricles, suggesting that the striolar domain is expanded, most probably owing to loss of RA (Fig. 7A,B; Ono et al., 2020). However, despite an increase in the striola-like domain in the macula of *Aldh1a3*$^{-/-}$ utricles, *Cyp26b1* expression was reduced in these mutants compared with controls (Fig. 7C,D). The reduced expression of *Cyp26b1* was detected in the cristae (Fig. 7C,D) and in the saccular macula (Fig. 7E,F). These results suggest that diminished RA signaling, as a consequence of the lack of *Aldh1a3*, causes the reduction in *Cyp26b1* expression. The *in vitro* upregulation of *Cyp26b1* by RA is also consistent with these results. Taking the *in vitro* and *in vivo* studies together, our results indicate that the expression of *Cyp26b1* transcripts is positively regulated by RA. The consequential low levels of RA determine the formation of the striolar/central zone rather than necessarily the *Cyp26b1* expression domain.

Timing of cell cycle exit is affected in mutants with misregulated RA signaling

Hair cell precursors in the striola exit from the cell cycle earlier than those in the extrastriola (Sans and Chat, 1982; Yang et al., 2017; Jiang et al., 2017). The striola is reduced in the *Cyp26b1*$^{-/-}$ and

Development (2020) 147, dev192070. doi:10.1242/dev.192070

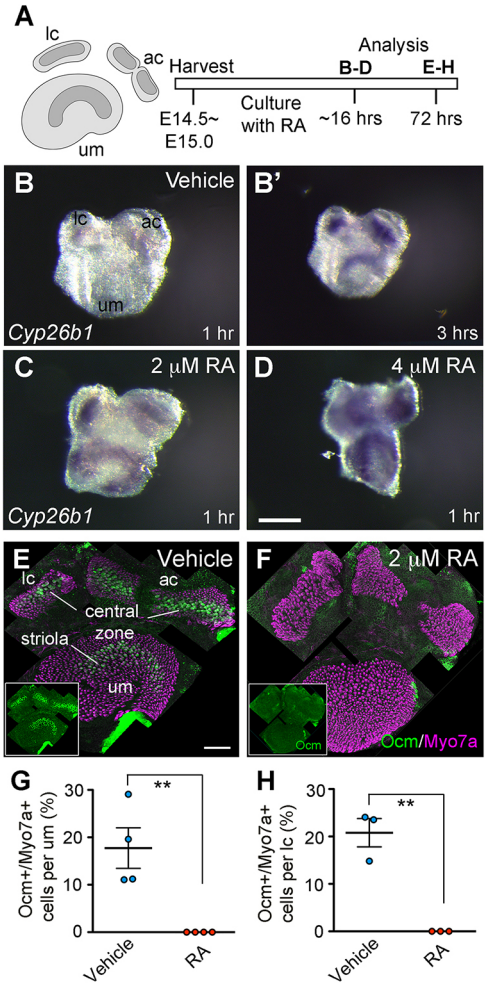

Fig. 6. Upregulation of *Cyp26b1* but reduction of Ocm by exogenous RA. (A) *In vitro* experimental design of RA treatments. Vestibular organs of E14.5-E15.0 mouse embryos were cultured in the presence of RA. Specimens were processed for *Cyp26b1 in situ* hybridization after 16 h or immunostaining after 72 h of culture. (B-D) In samples treated with 2 µM (C) or 4 µM (D) RA, utricular maculae (um), anterior (ac) and lateral (lc) cristae showed upregulated *Cyp26b1* transcripts in a dose-dependent manner (n=3 for each dose), in comparison to vehicle controls (n=4, B). Photographs of B-D were taken within 1 h after initiation of the *in situ* hybridization reaction. At this time, the reaction for the control sample (B) was incomplete; therefore, the hybridization reaction was extended to 3 h, and a photograph was taken (B′) at that time, which shows the normal *Cyp26b1* expression pattern. Notably, the *Cyp26b1* domain is expanded in RA-treated um. (E,F) Immunostaining of cultured vestibular organs with antibodies against Ocm (green) and Myo7a (magenta). (G,H) Quantification of percentages of Ocm$^+$ HCs. In controls, Ocm is expressed in type I HCs of the striola in um (17.7±4.3% per um, n=4; E,G) and the central zone in the lateral cristae (20.8±3.0% per lc, n=3; E,H). By contrast, Ocm$^+$ HCs are absent in RA-treated um (0%, n=4, P=0.0060, Student's unpaired t-test; F,G) and lateral cristae (0%, n=3, P=0.0023; F,H). Error bars: s.e.m. **P<0.01. Scale bars: 200 µm.

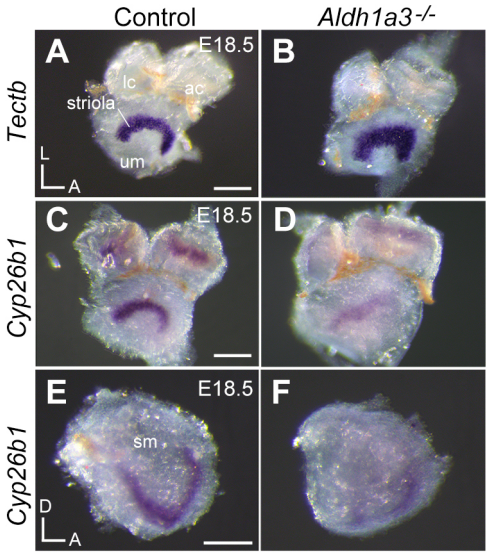

Fig. 7. Reduction of *Cyp26b1* in the vestibular organs of *Aldh1a3*$^{-/-}$ mice. (A,B) Whole mount *in situ* hybridization of *Tectb* transcripts in E18.5 mouse utricular maculae (um) and anterior (ac) and lateral cristae (lc). Absence of *Aldh1a3* in the um causes an increase in expression of *Tectb*, a gene expressed by striolar supporting cells (n=2 for each genotype). (C-F) Whole mount *in situ* hybridization of *Cyp26b1* transcripts in E18.5 vestibular organs. Despite the expanded striola based on *Tectb* expression patterns, *Cyp26b1* (which is also a normal striolar marker) is downregulated in the um, cristae (C,D, n=3) and saccular maculae (sm) (E,F, n=3) of *Aldh1a3*$^{-/-}$ mutants. Note the residual *Cyp26b1* signals in the vestibular organs of *Aldh1a3*$^{-/-}$ mutants. Orientations: A, anterior; D, dorsal; L, lateral. Scale bars: 200 µm.

expanded in the *Aldh1a3*$^{-/-}$ utricles. Therefore, we examined whether the timing of cell cycle exit is affected in maculae of *Cyp26b1*$^{-/-}$ and *Aldh1a3*$^{-/-}$ utricles by labeling with 5-ethynyl-2′-deoxyuridine (EdU; a thymidine analog). Timed pregnant dams were injected with EdU at E14.5, and embryos were harvested at E18.0. Cells with strong EdU labeling by E18.0 represent cells that have retained the EdU after incorporation at E14.5 without further dilution of EdU label between E14.5 and E18, suggesting that these cells have undergone terminal mitosis at or shortly after E14.5. Cells that are not labeled by EdU indicate either that they have exited from the cell cycle before EdU administration or that they have undergone repeated cell proliferation between E14.5 and E18, such that EdU labeling at E14.5 is diluted by cell division. In control utricular maculae, the central region was devoid of EdU labeling (Fig. 8A,A′), supporting previous reports that striolar cells are largely born by E14.5 (Yang et al., 2017; Jiang et al., 2017). This EdU-negative zone was reduced in the macula of *Cyp26b1*$^{-/-}$ and expanded in *Aldh1a3*$^{-/-}$ utricles (Fig. 8B-C′), suggesting a respective delay and premature terminal mitosis in the central region of the mutants, compared with controls. The change in the EdU-negative zone in these mutants is consistent with the reported respective loss and gain of striolar domain in *Cyp26b1*$^{-/-}$ and *Aldh1a3*$^{-/-}$ utricular maculae (Ono et al., 2020).

Next, we administered EdU to mutant dams earlier, at E11.5, and harvested at E18, in order to determine whether the increase in the EdU-negative zone in *Aldh1a3*$^{-/-}$ utricles was attributable to the extrastriolar region undergoing either premature cell cycle exit or increased proliferation such that the EdU labels were diluted. We reasoned that premature cell cycle exit in the extrastriolar region would be revealed by a higher number of EdU-labeled cells with an earlier EdU administration, when cells in the striola normally exit from the cell cycle. Compared with wild-type and heterozygous controls (Fig. 8E-E‴,G), *Aldh1a3*$^{-/-}$ utricular maculae injected with EdU at E11.5 indeed showed a higher number of EdU-labeled HCs that were co-labeled with the striolar HC marker Ocm at E18.0 (Fig. 8F-F‴,G). This suggests that more striolar-type I HCs were generated at E11.5 in *Aldh1a3*$^{-/-}$ mutants than in controls. Together, these results indicate that terminal differentiation in the central region of *Aldh1a3*$^{-/-}$ utricles is increased prematurely. Furthermore, these results suggest that RA signaling might control

Development (2020) 147, dev192070. doi:10.1242/dev.192070

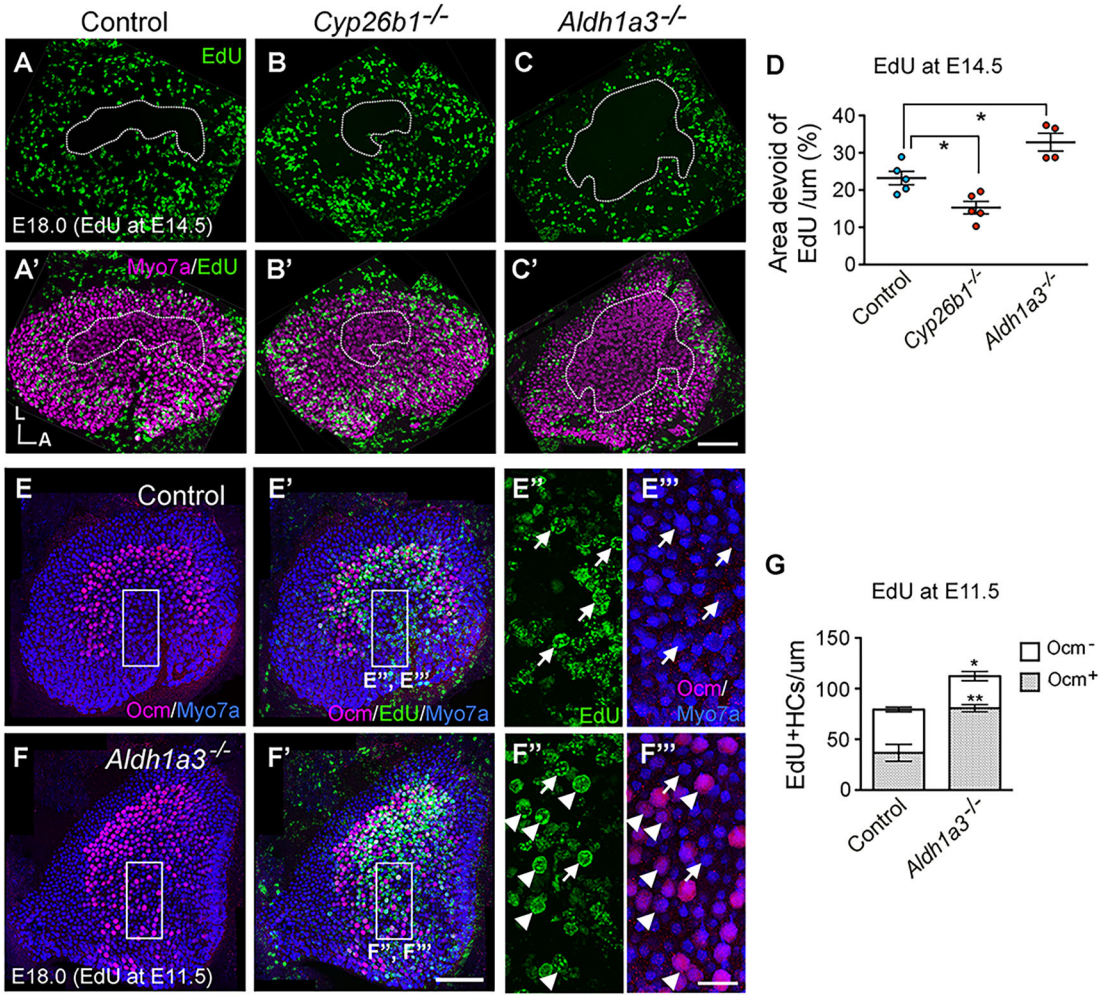

Fig. 8. Timing of cell cycle exit is affected in mutants with misregulated RA levels. (A-D) Immunohistochemistry (A-C′) and quantification (D) of myosin VIIA (Myo7a, magenta) and EdU labeling (green) of E18.0 utricular maculae (um) injected with EdU at E14.5. In control um, cells in the striola largely exited the cell cycle by E14.5 (A,A′, dotted outline; D, 23.2±1.7% of macular area, *n*=5). The area devoid of EdU is smaller in *Cyp26b1*$^{-/-}$ (B,B′, dotted outline; D, 15.2±1.7%, *n*=5, *P*=0.028) and larger in *Aldh1a3*$^{-/-}$ (C,C′, dotted outline; D, 32.8±2.4%, *n*=4, *P*=0.013) mutants, suggesting a reduced and expanded striolar region, respectively. (E-G) Immunohistochemistry of Myo7a (blue), oncomodulin (Ocm; magenta) and EdU (green) (E-F‴) and quantification of Ocm and EdU labeling (G) in HCs of E18.0 maculae that were injected with EdU at E11.5. (E-F′) Ocm and myosin VIIA staining (E,F) and merged Ocm, myosin VIIA and EdU labeling (E′,F′) of control (E,E′) and *Aldh1a3*$^{-/-}$ (F,F′) um. Magnified images of the rectangular area in the medial extrastriolar region (E,E′ or F,F′) are shown in E″,E‴ and F″,F‴, respectively. Arrowheads point to EdU^{+}/Ocm^{+} double positive HCs and arrows point to EdU^{+}/Ocm^{-} HCs. (G) Control maculae show a total of 79.3±9.1 EdU^{+} HCs, of which 36.7±7.5 cells are co-labeled with Ocm, indicating they are striolar type I HCs (G; *n*=3). *Aldh1a3*$^{-/-}$ mutant um show increased numbers of total EdU^{+} HCs (112.3±1.1 cells, *n*=3, *P*=0.032, Student's unpaired *t*-test), in addition to HCs that are both EdU^{+} and Ocm^{+} (80.7±3.2 cells, *P*=0.008), compared with controls. Error bars: s.e.m. One-way ANOVA with post-hoc Tukey's tests were applied for D. *P<0.05, **P<0.01. Orientations: A, anterior; L, lateral. Scale bars: 200 µm in C′ applies to A-C; 200 µm in F′ applies to E-F; 50 µm in F‴ applies to E″-F″.

the timing of cell cycle exit by stimulating cell proliferation in embryonic vestibular epithelia.

DISCUSSION

RDH10 generates the substrate for ALDH1a3 in vestibular development

Previous studies have demonstrated that wild-type expression of *Aldh1a3* is required for the separation of the utricle and saccule, formation of otoconia and patterning of otolithic organs (Ono et al., 2020; Romand et al., 2013). These requirements are similar to those reported here for *Rdh10* (Figs 3-5), suggesting that RDH10 catalyzes production of the substrate, retinaldehyde, required by ALDH1a3 for inner ear development (Fig. 9A). The loss of otoconial formation in *Aldh1a3* mutants is attributed to the reduced gene expression of *Otop1* (Romand et al., 2013), which is mutated in the *tilted* mice, and this mutant shows a similar otoconial phenotype to *Aldh1a3* mutants (Hurle et al., 2003; Ornitz et al., 1998). The similarity in otoconial phenotype between *Aldh1a3* and *Rdh10* also suggests that RA is required for otoconia formation.

In contrast to *Aldh1a3*$^{-/-}$ ears, in which only the striola was affected but not the central zone of the cristae, our study showed that both the striola and the central zones were affected by deletion of *Rdh10*. This suggests that there is a compensatory mechanism for RA production by other ALDH1a enzymes in crista patterning (Fig. 9B).

Recent findings showed that *Cyp26b1* is expressed in the striolar/central zone of all vestibular sensory organs, and features of the striolar/central zone are lost in *Cyp26b1* conditional knockouts (Ono et al., 2020). We had proposed that formation of the striolar/central zone of vestibular organs requires *Cyp26b1*-mediated

Development (2020) 147, dev192070. doi:10.1242/dev.192070

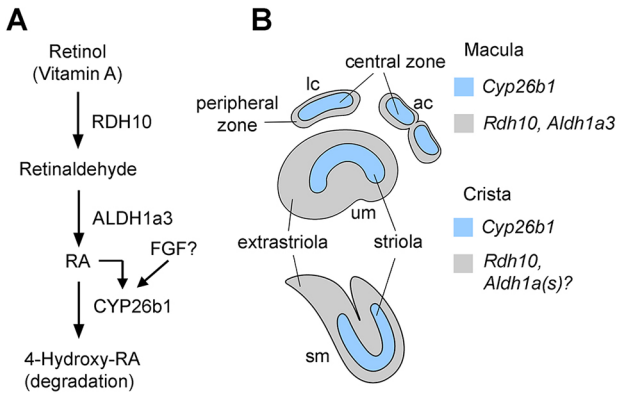

Fig. 9. Retinoic acid signaling pathway in patterning of vestibular organs. (A) Summary of RA signaling pathway required for zonal patterning of vestibular organs. (B) A diagram illustrating the genes required for patterning individual zones of the vestibular organs. ac, anterior crista; lc, lateral crista; sm, saccular macula; um, utricular macula.

reduction of RA levels. The phenotypes of *Cyp26b1*$^{-/-}$ and *Rdh10* cKO mutants are opposite and consistent with each other: a reduction versus an expansion of the striolar/central zone, respectively. These results strongly argue that patterning of the vestibular organs is regulated by RA signaling. Notably, the maculae of both *Aldh1a3*$^{-/-}$ and *Rdh10* cKO utricles show an expansion of Ocm expression in the medial but not in the lateral extrastriola (Fig. 5; Ono et al., 2020). In the saccular macula, Ocm expression expands to both sides of the striola (Fig. 5). Although the differences in Ocm expansion between the two maculae might be related to their intrinsic differences in striolar-LPR relationship, the underlying molecular mechanisms that generated these regional differences are not clear. Notably, there are molecular and cellular differences that set the lateral extrastriola in the utricular macula apart from the medial extrastriola (Jiang et al., 2017). It is likely that another mechanism (or mechanisms) in addition to RA might function in patterning the lateral extrastriola and affects their response to a reduction in RA signaling. Alternatively, and not mutually exclusive, other ADH/RDH and ALDH1a enzymes might have redundant functions for specification of the lateral extrastriola. Indeed, *Adh4*, *Aldh1a1* and *Aldh1a2* are known to be expressed in the inner ear during embryogenesis (Haselbeck and Duester, 1998; Romand et al., 2004).

Cyp26b1 expression is regulated by RA signaling

By combining genetic and *in vitro* analyses, we showed that *Cyp26b1* expression in the vestibular organs is under the control of RA signaling. Notably, in *Aldh1a3*$^{-/-}$ mutants, striolar markers, such as Ocm and Tectb, were increased beyond the reduced *Cyp26b1* domain, which normally demarcates the prospective striolar/central zone (Fig. 7; Ono et al., 2020). Likewise, after RA treatment of utricular macula explants, Ocm expression was absent despite upregulation of *Cyp26b1* (Fig. 6). Together, these results suggest that formation of the striola and central zones is dependent upon the absence or reduction of RA levels, rather than the expression domain of *Cyp26b1* per se.

The expression of Cyp26 genes is regulated by RA in various species, including non-chordates (Ishibashi et al., 2005; Reijntjes et al., 2005; Tanibe et al., 2008; White et al., 2007). The transcriptional regulation of *Cyp26a1* is mediated by a conserved RARE element in the *Cyp26a1* promoter, to which RA and the RAR/RXR heterodimers can bind (Loudig et al., 2000; Ross and Zolfaghari, 2011). By contrast, *Cyp26b1* lacks a RARE in its proximal regulatory region, and therefore, *Cyp26b1* regulation by RA is likely to be indirect.

Our results showed that *Cyp26b1* expression in the vestibular organs is not abolished by deletion of *Aldh1a3* (Fig. 7C-F). Residual *Cyp26b1* expression might simply be induced by the remaining RA secreted from surrounding non-sensory epithelia expressing other *Aldh1a* genes. Alternatively, other factors might be involved in the regulation of *Cyp26b1*. This idea is supported by previous findings that although the expression patterns of all three *Cyp26b* genes are affected in vitamin A-deficient quails, some expression domains remained unchanged (Reijntjes et al., 2005). Similar effects were observed in zebrafish treated with an RA inhibitor (White et al., 2007). Therefore, it is possible that the residual *Cyp26b1* expression in the striolar/central zone in *Aldh1a3* mutants is regulated by other positional cues in the developing vestibular organs. Likely regulators could be fibroblast growth factors (FGFs; Fig. 9A), because cross-regulation of RA and FGF signaling pathways is common in developing systems (Cunningham and Duester, 2015). Several FGF ligands, including FGF10 and FGF20, are expressed in the vestibular organs (Huh et al., 2012; Pauley et al., 2003). However, whether these FGF ligands regulate *Cyp26b1* expression will require further investigation. Nevertheless, RA functions as an inducer of *Cyp26b1*, which ensures proper formation of the striolar/central zone (Fig. 9A).

RA signaling regulates cell proliferation

Unlike the cochlea, vestibular organs retain the ability to restore lost HCs, in part, through re-entry of postmitotic supporting cells into the cell cycle and subsequent differentiation into HCs (Burns and Stone, 2017). RA signaling might be an inducer of supporting cell re-entry into the cell cycle. Our results showed that augmentation of RA signaling by removal of *Cyp26b1* causes prolonged cell proliferation, whereas reduction of RA in *Aldh1a3*$^{-/-}$ mutants promotes premature cell cycle exit of HC progenitors (Fig. 8). These phenotypes might be attributed to direct regulation of the cell cycle by altered RA signaling. Alternatively, the effects of RA signaling on the cell cycle progression might be secondary to regional specification of the sensory organs. The former possibility is supported by findings that RA signaling is required for mitotic HC regeneration in zebrafish inner ear and neuromasts (Rubbini et al., 2015). Notably, in these organs, the components of the RA signaling pathway, such as *Aldh1a3*, *Cyp26b1* and *Rarga*, which encodes an RA receptor, are induced upon damage to the HCs. Elucidation of the mechanisms by which RA signaling mediators are regulated during HC regeneration in mammalian vestibular organs is important if RA is to be developed as a potential therapeutic agent to alleviate hearing loss and balance disorders.

MATERIALS AND METHODS

Mice

Mouse strains used in the study were as follows: *Cyp26b1*$^{+/-}$ (Ono et al., 2020), *Aldh1a3*$^{+/-}$ maintained in a mixed C57BL/6J and CD1 background (Molotkov et al., 2006), *Rdh10*$^{flox/flox}$ and *Rdh10*$^{+/-}$ both maintained in a C57BL/6J background (Sandell et al., 2012), and *Foxg1*^{Cre} maintained in a C57BL/6J background (Hébert and McConnell, 2000; RRID: IMSR_JAX:004337). *Foxg1*^{Cre}; *Rdh10*$^{flox/-}$ were generated by crossing *Foxg1*^{Cre}; *Rdh10*$^{+/-}$ males with *Rdh10*$^{flox/flox}$ females, and embryos were collected prenatally because mutants die after birth. Either males or females were used in this study. All animal experiments were conducted according to US National Institutes of Health animal user guidelines under the approved animal protocol NIH 1212-20 and the Stowers Institute for Medical Research IACUC protocol 2019-097.

Genotyping and tissue preparation

Genotyping for the *Cyp26b1*$^{+/-}$, *Aldh1a3*$^{+/-}$, *Rdh10*$^{+/-}$ and *Rdh10*^{lox} alleles was performed by Transnetyx, based on sequence information described

Development (2020) 147, dev192070. doi:10.1242/dev.192070

previously (Ono et al., 2020; Sandell et al., 2012). Timed pregnant females were euthanized, and embryos were harvested as indicated. Hemi-sectioned heads of the embryos were fixed in 4% paraformaldehyde overnight. Then, fixed samples were cryoprotected with 30% sucrose and stored at −80°C until processing for cryosectioning or whole mount dissections.

In situ hybridization

In situ hybridization was conducted as previously described (Morsli et al., 1998). Digoxigenin-labeled RNA probes were generated for mouse *Cyp26b1* (GenBank: AW049789) and *Tectb* (Rau et al., 1999) as described. To enhance the detection of *Rdh10* transcripts in the inner ear, two RNA probes were used simultaneously, an antisense probe hybridizing to the 5′ end of the *Rdh10* complementary DNA (cDNA) as described by Sandell et al. (2007) and one hybridizing to the 3′ untranslated region of the cDNA. This 3′ probe is 769 bp in length, generated using PCR with a *Rdh10* cDNA and the forward and reverse primers CGACAGTGTAGTGCTCTGTTGT and TCTTTAGAAA-ACATCCCGATTTG, respectively.

Whole mount immunohistochemistry

Dissected saccular maculae or utricular maculae with anterior and lateral cristae attached were blocked with PBS containing 4% normal donkey serum and 0.2% Triton X-100 (PBT). Then, specimens were transferred to blocking buffer with primary antibodies and incubated overnight at 4°C. The primary antibodies used were as follows: goat polyclonal anti-oncomodulin (1:300, Santa Cruz Biotech, sc-7446), rabbit polyclonal anti-myosin VIIA (1:1000, Proteus, 25-6790) and mouse anti-βII-spectrin (1:500, BD Bioscience, 612562). After extensive washing with PBT, specimens were incubated with appropriate secondary antibodies conjugated with fluorescent proteins: donkey anti-mouse, anti-rabbit or anti-goat IgG (H+L) antibody (1:500, Thermo Fisher Scientific, A32744, A32754 or A32814). Samples were then washed and mounted in ProLong Gold Antifade (Invitrogen). Images were obtained by using a Zeiss LSM780 confocal microscope and automatically tiled with Photoshop software.

Paint fill

Paint filling was conducted as described previously (Morsli et al., 1998). Briefly, heads of E16.5 embryos were fixed with Bodian's fixative overnight at room temperature, followed by dehydration with ethanol and clearance with methyl salicylate. Using a pulled glass capillary tube attached to a Hamilton syringe, 0.01% of either alkyd enamel paint or correction fluid in methyl salicylate was micro-injected into the middle turn of the cochlear duct. For control samples after E15.5, in which the utricle and saccule were separated, another injection was delivered to the utricle to fill the remaining membranous labyrinth.

Retinoic acid preparation and treatments of vestibular organs *in vitro*

All-*trans*-RA powder (Sigma-Aldrich, #R2625) was dissolved in 100% ethanol at a concentration of 5 mg/ml. The prepared stock solution was stored at −80°C until use. Timed pregnant CD1 females were harvested when embryos reached E14.5-E15.0. Inner ear tissues, composed of the utricular macula and the anterior and lateral cristae, were promptly dissected in cold PBS and maintained on ice. For determination of Ocm expression, dissected vestibular organs were transferred to Millicell culture inserts (Millipore Sigma, #PIHP01250) with the sensory epithelium facing up, and each insert was placed into a well of a 24-well plate containing ∼200 µl of the culture medium DMEM (Gibco, #12430-054) with 100 U/ml of penicillin G potassium salt (Sigma Aldrich, #P7794) and RA at a final concentration of 2 µM when indicated. Specimens were incubated in a humidified atmosphere of 95% air and 5% CO_2 for 72 h. After incubation, specimens were fixed in 4% paraformaldehyde at room temperature for 15 min. Then, the membrane of the Millicell insert with the fixed tissue attached was removed from the vehicle and processed for immunostaining as a unit. After immunostaining, explants were carefully removed from the membrane and transferred to a glass slide for mounting and imaging.

For analysis of *Cyp26b1* transcripts, dissected specimens were free-floated in a 24-well plate containing 400 µl of culture medium with penicillin G and 2 or 4 µM RA as indicated. Cultures were incubated overnight before fixing with 4% paraformaldehyde for 15 min, washed and stored in 50% methanol at −20°C until subsequent processing for whole mount *in situ* hybridization.

EdU administration and imaging

Pregnant females were injected with EdU (1 mg/ml solution in PBS; Thermo Fisher Scientific) intraperitoneally at E11.5 or E14.5 at a dose of 10 µg EdU/g of body weight, and all embryos were harvested at E18.5 and fixed with 4% paraformaldehyde. After utricular maculae were dissected and immunostained with anti-myosin VIIa and anti-Ocm antibodies, EdU-labeled cells were visualized using a Click-iT EdU Alexa Fluor 488 imaging kit (Thermo Fisher Scientific).

Acknowledgements

We thank Drs Lisa Cunningham and Thomas Friedman, and members of our laboratory for critical reading of the manuscript. We also thank Michael Mulheisen for conducting *in situ* hybridization experiments.

Competing interests

The authors declare no competing or financial interests.

Author contributions

Conceptualization: K.O., D.K.W.; Methodology: K.O., D.K.W.; Formal analysis: K.O.; Investigation: K.O.; Resources: L.L.S., P.A.T.; Data curation: K.O.; Writing - original draft: K.O.; Writing - review & editing: K.O., L.L.S., P.A.T., D.K.W.; Supervision: D.K.W.; Project administration: D.K.W.; Funding acquisition: P.A.T., D.K.W.

Funding

This research was supported by funds from the intramural program at the National Institute on Deafness and Other Communication Disorders (D.K.W.) and by the National Institute for Dental and Craniofacial Research (DE016082 to P.A.T.) and the Stowers Institute for Medical Research (P.A.T.). Deposited in PMC for release after 12 months.

Data availability

All data are available from the corresponding author upon reasonable request.

Peer review history

The peer review history is available online at https://dev.biologists.org/lookup/doi/10.1242/dev.192070.reviewer-comments.pdf

References

Anderson, E. L., Baltus, A. E., Roepers-Gajadien, H. L., Hassold, T. J., de Rooij, D. G., van Pelt, A. M. M. and Page, D. C. (2008). Stra8 and its inducer, retinoic acid, regulate meiotic initiation in both spermatogenesis and oogenesis in mice. *Proc. Natl. Acad. Sci. USA* **105**, 14976-14980. doi:10.1073/pnas.0807297105

Bok, J., Raft, S., Kong, K.-A., Koo, S. K., Dräger, U. C. and Wu, D. K. (2011). Transient retinoic acid signaling confers anterior-posterior polarity to the inner ear. *Proc. Natl. Acad. Sci. USA* **108**, 161-166. doi:10.1073/pnas.1010547108

Burns, J. C. and Stone, J. S. (2017). Development and regeneration of vestibular hair cells in mammals. *Semin. Cell Dev. Biol.* **65**, 96-105. doi:10.1016/j.semcdb.2016.11.001

Cantos, R., Cole, L. K., Acampora, D., Simeone, A. and Wu, D. K. (2000). Patterning of the mammalian cochlea. *Proc. Natl. Acad. Sci. USA* **97**, 11707-11713. doi:10.1073/pnas.97.22.11707

Cunningham, T. J. and Duester, G. (2015). Mechanisms of retinoic acid signalling and its roles in organ and limb development. *Nat. Rev. Mol. Cell Biol.* **16**, 110-123. doi:10.1038/nrm3932

da Silva, S. and Cepko, C. L. (2017). Fgf8 expression and degradation of retinoic acid are required for patterning a high-acuity area in the retina. *Dev. Cell* **42**, 68-81.e6. doi:10.1016/j.devcel.2017.05.024

Duester, G. (2008). Retinoic acid synthesis and signaling during early organogenesis. *Cell* **134**, 921-931. doi:10.1016/j.cell.2008.09.002

Eatock, R. A. and Songer, J. E. (2011). Vestibular hair cells and afferents: two channels for head motion signals. *Annu. Rev. Neurosci.* **34**, 501-534. doi:10.1146/annurev-neuro-061010-113710

Farjo, K. M., Moiseyev, G., Nikolaeva, O., Sandell, L. L., Trainor, P. A. and Ma, J.-X. (2011). RDH10 is the primary enzyme responsible for the first step of embryonic Vitamin A metabolism and retinoic acid synthesis. *Dev. Biol.* **357**, 347-355. doi:10.1016/j.ydbio.2011.07.011

Haselbeck, R. J. and Duester, G. (1998). ADH4-lacZ transgenic mouse reveals alcohol dehydrogenase localization in embryonic midbrain/hindbrain, otic

vesicles, and mesencephalic, trigeminal, facial, and olfactory neural crest. *Alcohol. Clin. Exp. Res.* **22**, 1607-1613. doi:10.1111/j.1530-0277.1998.tb03955.x

Hébert, J. M. and McConnell, S. K. (2000). Targeting of cre to the Foxg1 (BF-1) locus mediates loxP recombination in the telencephalon and other developing head structures. *Dev. Biol.* **222**, 296-306. doi:10.1006/dbio.2000.9732

Hernandez, R. E., Putzke, A. P., Myers, J. P., Margaretha, L. and Moens, C. B. (2007). Cyp26 enzymes generate the retinoic acid response pattern necessary for hindbrain development. *Development* **134**, 177-187. doi:10.1242/dev.02706

Huh, S.-H., Jones, J., Warchol, M. E. and Ornitz, D. M. (2012). Differentiation of the lateral compartment of the cochlea requires a temporally restricted FGF20 signal. *PLoS Biol.* **10**, e1001231. doi:10.1371/journal.pbio.1001231

Hurle, B., Ignatova, E., Massironi, S. M., Mashimo, T., Rios, X., Thalmann, I., Thalmann, R. and Ornitz, D. M. (2003). Non-syndromic vestibular disorder with otoconial agenesis in tilted/mergulhador mice caused by mutations in otopetrin 1. *Hum. Mol. Genet.* **12**, 777-789. doi:10.1093/hmg/ddg087

Ishibashi, T., Usami, T., Fujie, M., Azumi, K., Satoh, N. and Fujiwara, S. (2005). Oligonucleotide-based microarray analysis of retinoic acid target genes in the protochordate, Ciona intestinalis. *Dev. Dyn.* **233**, 1571-1578. doi:10.1002/dvdy.20486

Jacobs, S., Lie, D. C., DeCicco, K. L., Shi, Y., DeLuca, L. M., Gage, F. H. and Evans, R. M. (2006). Retinoic acid is required early during adult neurogenesis in the dentate gyrus. *Proc. Natl. Acad. Sci. USA* **103**, 3902-3907. doi:10.1073/pnas.0511294103

Jiang, T., Kindt, K. and Wu, D. K. (2017). Transcription factor Emx2 controls stereociliary bundle orientation of sensory hair cells. *eLife* **6**, e23661. doi:10.7554/elife.23661

Jones, T. A., Lee, C., Gaines, G. C. and Grant, J. W. W. (2015). On the high frequency transfer of mechanical stimuli from the surface of the head to the macular neuroepithelium of the mouse. *J. Assoc. Res. Otolaryngol.* **16**, 189-204. doi:10.1007/s10162-014-0501-9

Kumar, S., Sandell, L. L., Trainor, P. A., Koentgen, F. and Duester, G. (2012). Alcohol and aldehyde dehydrogenases: retinoid metabolic effects in mouse knockout models. *Biochim. Biophys. Acta* **1821**, 198-205. doi:10.1016/j.bbalip.2011.04.004

Loudig, O., Babichuk, C., White, J., Abu-Abed, S., Mueller, C. and Petkovich, M. (2000). Cytochrome P450RAI(CYP26) promoter: a distinct composite retinoic acid response element underlies the complex regulation of retinoic acid metabolism. *Mol. Endocrinol.* **14**, 1483-1497. doi:10.1210/mend.14.9.0518

McInturff, S., Burns, J. C. and Kelley, M. W. (2018). Characterization of spatial and temporal development of type I and type II hair cells in the mouse utricle using new cell-type-specific markers. *Biol. Open* **7**, bio038083. doi:10.1242/bio.038083

Metzler, M. A. and Sandell, L. L. (2016). Enzymatic metabolism of vitamin A in developing vertebrate embryos. *Nutrients* **8**, 812. doi:10.3390/nu8120812

Molotkov, A., Molotkova, N. and Duester, G. (2006). Retinoic acid guides eye morphogenetic movements via paracrine signaling but is unnecessary for retinal dorsoventral patterning. *Development* **133**, 1901-1910. doi:10.1242/dev.02328

Morsli, H., Choo, D., Ryan, A., Johnson, R. and Wu, D. K. (1998). Development of the mouse inner ear and origin of its sensory organs. *J. Neurosci.* **18**, 3327-3335. doi:10.1523/JNEUROSCI.18-09-03327.1998

Ono, K., Keller, J., López Ramírez, O., González Garrido, A., Zobeiri, O. A., Chang, H. H. V., Vijayakumar, S., Ayiotis, A., Duester, G., Della Santina, C. C. et al. (2020). Retinoic acid degradation shapes zonal development of vestibular organs and sensitivity to transient linear accelerations. *Nat. Commun.* **11**, 63. doi:10.1038/s41467-019-13710-4

Ornitz, D. M., Bohne, B. A., Thalmann, I., Harding, G. W. and Thalmann, R. (1998). Otoconia agenesis in tilted mutant mice. *Hear. Res.* **122**, 60-70. doi:10.1016/S0378-5955(98)00080-X

Paffenholz, R., Bergstrom, R. A., Pasutto, F., Wabnitz, P., Munroe, R. J., Jagla, W., Heinzmann, U., Marquardt, A., Bareiss, A., Laufs, J. et al. (2004). Vestibular defects in head-tilt mice result from mutations in Nox3, encoding an NADPH oxidase. *Genes Dev.* **18**, 486-491. doi:10.1101/gad.1172504

Pauley, S., Wright, T. J., Pirvola, U., Ornitz, D., Beisel, K. and Fritzsch, B. (2003). Expression and function of FGF10 in mammalian inner ear development. *Dev. Dyn.* **227**, 203-215. doi:10.1002/dvdy.10297

Rau, A., Legan, P. K. and Richardson, G. P. (1999). Tectorin mRNA expression is spatially and temporally restricted during mouse inner ear development. *J. Comp. Neurol.* **405**, 271-280. doi:10.1002/(SICI)1096-9861(19990308)405:2<271::AID-CNE10>3.0.CO;2-2

Reijntjes, S., Blentic, A., Gale, E. and Maden, M. (2005). The control of morphogen signalling: regulation of the synthesis and catabolism of retinoic acid in the developing embryo. *Dev. Biol.* **285**, 224-237. doi:10.1016/j.ydbio.2005.06.019

Rhinn, M., Schuhbaur, B., Niederreither, K. and Dolle, P. (2011). Involvement of retinol dehydrogenase 10 in embryonic patterning and rescue of its loss of function by maternal retinaldehyde treatment. *Proc. Natl. Acad. Sci. USA* **108**, 16687-16692. doi:10.1073/pnas.1103877108

Romand, R., Niederreither, K., Abu-Abed, S., Petkovich, M., Fraulob, V., Hashino, E. and Dolle, P. (2004). Complementary expression patterns of retinoid acid-synthesizing and -metabolizing enzymes in pre-natal mouse inner ear structures. *Gene Expr. Patterns* **4**, 123-133. doi:10.1016/j.modgep.2003.09.006

Romand, R., Kondo, T., Cammas, L., Hashino, E. and Dolle, P. (2008). Dynamic expression of the retinoic acid-synthesizing enzyme retinol dehydrogenase 10 (rdh10) in the developing mouse brain and sensory organs. *J. Comp. Neurol.* **508**, 879-892. doi:10.1002/cne.21707

Romand, R., Krezel, W., Beraneck, M., Cammas, L., Fraulob, V., Messaddeq, N., Kessler, P., Hashino, E. and Dolle, P. (2013). Retinoic acid deficiency impairs the vestibular function. *J. Neurosci.* **33**, 5856-5866. doi:10.1523/JNEUROSCI.4618-12.2013

Ross, A. C. and Zolfaghari, R. (2011). Cytochrome P450s in the regulation of cellular retinoic acid metabolism. *Annu. Rev. Nutr.* **31**, 65-87. doi:10.1146/annurev-nutr-072610-145127

Ross, S. A., McCaffery, P. J., Drager, U. C. and De Luca, L. M. (2000). Retinoids in embryonal development. *Physiol. Rev.* **80**, 1021-1054. doi:10.1152/physrev.2000.80.3.1021

Rubbini, D., Robert-Moreno, A., Hoijman, E. and Alsina, B. (2015). Retinoic acid signaling mediates hair cell regeneration by repressing p27kip and sox2 in supporting cells. *J. Neurosci.* **35**, 15752-15766. doi:10.1523/JNEUROSCI.1099-15.2015

Sakai, Y., Meno, C., Fujii, J., Nishino, J., Shiratori, H., Saijoh, Y., Rossant, J. and Hamada, H. (2001). The retinoic acid-inactivating enzyme CYP26 is essential for establishing an uneven distribution of retinoic acid along the anterio-posterior axis within the mouse embryo. *Genes Dev.* **15**, 213-225. doi:10.1101/gad.851501

Sandell, L. L., Sanderson, B. W., Moiseyev, G., Johnson, T., Mushegian, A., Young, K., Rey, J.-P., Ma, J.-X., Staehling-Hampton, K. and Trainor, P. A. (2007). RDH10 is essential for synthesis of embryonic retinoic acid and is required for limb, craniofacial, and organ development. *Genes Dev.* **21**, 1113-1124. doi:10.1101/gad.1533407

Sandell, L. L., Lynn, M. L., Inman, K. E., McDowell, W. and Trainor, P. A. (2012). RDH10 oxidation of vitamin A is a critical control step in synthesis of retinoic acid during mouse embryogenesis. *PLoS ONE* **7**, e30698. doi:10.1371/journal.pone.0030698

Sans, A. and Chat, M. (1982). Analysis of temporal and spatial patterns of rat vestibular hair cell differentiation by tritiated thymidine radioautography. *J. Comp. Neurol.* **206**, 1-8. doi:10.1002/cne.902060102

Simmons, D. D., Tong, B., Schrader, A. D. and Hornak, A. J. (2010). Oncomodulin identifies different hair cell types in the mammalian inner ear. *J. Comp. Neurol.* **518**, 3785-3802. doi:10.1002/cne.22424

Tanibe, M., Michiue, T., Yukita, A., Danno, H., Ikuzawa, M., Ishiura, S. and Asashima, M. (2008). Retinoic acid metabolizing factor xCyp26c is specifically expressed in neuroectoderm and regulates anterior neural patterning in Xenopus laevis. *Int. J. Dev. Biol.* **52**, 893-901. doi:10.1387/ijdb.082683mt

White, R. J., Nie, Q., Lander, A. D. and Schilling, T. F. (2007). Complex regulation of cyp26a1 creates a robust retinoic acid gradient in the zebrafish embryo. *PLoS Biol.* **5**, e304. doi:10.1371/journal.pbio.0050304

Yang, X., Qian, X., Ma, R., Wang, X., Yang, J., Luo, W., Chen, P., Chi, F. and Ren, D. (2017). Establishment of planar cell polarity is coupled to regional cell cycle exit and cell differentiation in the mouse utricle. *Sci. Rep.* **7**, 43021. doi:10.1038/srep43021

Yashiro, K., Zhao, X., Uehara, M., Yamashita, K., Nishijima, M., Nishino, J., Saijoh, Y., Sakai, Y. and Hamada, H. (2004). Regulation of retinoic acid distribution is required for proximodistal patterning and outgrowth of the developing mouse limb. *Dev. Cell* **6**, 411-422. doi:10.1016/S1534-5807(04)00062-0